ChemistrySelect

Research Article
doi.org/10.1002/slct.202403339

Chemistry Europe
European Chemical Societies Publishing

www.chemistryselect.org

Enhanced Photodegradation of Imidacloprid Using ZnO@Ca-Alginate Composites: Optimization of pH and pHzcp for Effective Water Treatment

Ahlam Zyoud,[a] Ahed H. Zyoud,*[a] Shaher H. Zyoud,[b] Samer H. Zyoud,[c] Naser Qamhieh,[d] and Hikmat S. Hilal[a]

This research focused on the photodegradation of the insecticide imidacloprid (IM) via a ZnO@Ca-Alginate composite catalyst to address water contamination issues, particularly in agricultural areas such as Palestine. The composite was synthesized and characterized by scanning electron microscopy (SEM), X-ray diffraction (XRD), energy dispersive X-ray (EDX), thermogravimetric analysis (TGA), and Fourier transform infrared (FT-IR) spectroscopy, confirming the presence of ZnO. Photocatalytic experiments under simulated solar light revealed significant IM degradation, with a 50% reduction in 40 minutes, an 80% reduction in 2 hours, and up to 94% in 3 hours. The degradation efficiency was influenced by the point of zero charge (pHzcp) and solution pH, with optimal performance under neutral to slightly basic conditions. UV-visible spectrophotometry, high-performance liquid chromatography (HPLC), and total organic carbon (TOC) analyses verified complete IM mineralization, yielding CO_2, Cl^-, and NO_3^- after 3 hours. The ZnO@Ca-Alginate composite demonstrated high reusability, highlighting its potential for treating pesticide-contaminated water. This study emphasizes the need for efficient pollutant removal technologies in regions where agricultural pollutants are prevalent.

1. Introduction

The contamination of water sources by several organic pollutants, including herbicides, pesticides, insecticides, pharmaceuticals, and dyes, constitutes a significant threat to the environment worldwide.[1,2] The World Health Organization (WHO) recognized drinking water contamination as a global issue, particularly across developing countries, where over 2 million people die yearly because of a shortage of clean and safe drinking water.[3,4] In this context, purifying techniques, which include biological, chemical, and physical treatments such as adsorption,[5–7] have emerged to mitigate water contaminants.[8] Considering their efficacy in reducing water contaminants, advanced methods that include adsorption, sedimentation, precipitation, filtration, ion exchange, chlorination, and oxidation often encounter deficiencies, compelling the emergence of novel technologies.[9,10] Among these developed technologies, composite adsorbents that incorporate solid substrates along with photocatalyst semiconductor nanoparticles have emerged as potential solutions.[7,11–15] These composite materials promote organic contaminant elimination via adsorption and photodegradation, enabling improved water treatment, particularly for the elimination of water organic contaminants.

A key advancement presented in this study is the development of a ZnO@Ca-Alginate composite that synergistically combines adsorption and photodegradation for the effective removal of imidacloprid (IM). This innovative approach enhances the efficiency of IM removal by leveraging the strengths of both mechanisms in a single system. Imidacloprid was specifically chosen for this study because of its widespread agricultural use and persistent presence in water bodies, which poses significant environmental risks, particularly to aquatic ecosystems and pollinators.[16] Its stability across varying pH levels and resistance to conventional water treatment methods make it an ideal candidate for demonstrating the efficiency of our composite material.[17,18] The composite's dual functionality not only provides an effective strategy for addressing organic pollutants such as imidacloprid but also presents a promising and more efficient alternative to traditional methods, making it a valuable solution for large-scale water treatment applications. In addition to its technical advantages, the ZnO@Ca-Alginate composite offers a cost-effective solution for water treatment. Its fabrication uses low-cost, widely available materials such as zinc oxide and alginate, resulting in significantly lower production costs than those of conventional methods. The composite's dual-functionality eliminates the need for separate treatment stages, thus decreasing operational expenses. This economic viability, coupled with its high efficacy in organic pollutant removal, positions the ZnO@Ca-Alginate composite as

[a] A. Zyoud, A. H. Zyoud, H. S. Hilal
SSERL, Chemistry Department, An-Najah National University, Nablus, State of Palestine
00970599353404
E-mail: ahedzyoud@najah.edu

[b] S. H. Zyoud
Department of Building Engineering and Environment, Palestine Technical University (Kadoorie), Tulkarm, State of Palestine

[c] S. H. Zyoud
Department of Mathematics and Sciences, Ajman University, P.O. Box 346, Ajman, United Arab Emirates

[d] N. Qamhieh
Department of Physics, United Arab Emirates University, Al-Ain, United Arab Emirates

an attractive option for large-scale water treatment applications.

The use of semiconductor nanoparticles in photodegradation methods employing semiconductor photocatalysts has significant potential for effectively mineralizing organic contaminants in contaminated water.[19–22] Composite systems exhibit optimized adsorption and photodegradation efficiency.[23–25] The synergistic adsorption and photodegradation efficiencies of composites are strongly related to the solution pH and the surface charge of the composite.[26–30] The photodegradation of organic contaminants in water is initiated by the absorption of a proper photon by a semiconductor nanoparticle, exciting a portion of the electrons in the valence band up to the conduction spectrum while releasing a positive hole (h^+) in the valence band. The positive holes produced can oxidize adjacent molecules such as H_2O, OH^-, and O_2, generating highly reactive hydroxyl radicals ($OH^•$) that are responsible for degrading organic pollutants.[30–32]

Among semiconductor photocatalysts, zinc oxide (ZnO) is a nontoxic, highly effective option. Owing to its substantial binding energy of 60 MeV and band gap of ~3.2 eV, ZnO exhibits superior UV absorption properties compared with those of other stable semiconductors (e.g., titanium dioxide; TiO_2). This characteristic makes it particularly advantageous for photocatalytic applications, especially considering that the UV fraction is only approximately 4% of the reach in solar light.[33–36]

In the case of such composite systems, semiconductor nanoparticles play a substantial role in the photodegradation of organic and chemical pollutants. These substrate composites facilitate the recovery and reuse of the photocatalyst while enhancing pollution molecule adsorption on the photocatalyst composite surface, which improves the efficiency of photodegradation.[35] Various materials, including activated carbon, clay derivatives, ceramics, and sands, have been explored as substrates for photocatalysts. Alginate, derived from alginic acid, has been extensively used for the adsorption of organic water continents.[37–39] Alginate has emerged as a particularly promising substrate because of its natural, nontoxic nature and ability to form insoluble gelatin beads, known as calcium alginate, when cross-linked with calcium ions (Figure 1).[40–42] Alginate-supported ZnO and TiO_2 have demonstrated effectiveness in adsorption-based water contaminant removal, surpassing other materials in this regard. However, the use of ZnO@Ca-Alginate composite materials for photodegradation remains relatively unexplored, particularly compared with studies on other pollutants, such as aqueous methylene blue,[12] or other early reports on the limited photodegradation of organic contaminants utilizing ZnO as a photocatalyst incorporated within the composite or other semiconductors embedded in the composite.[43–46] Nevertheless, preliminary investigations suggest promising results in enhancing catalyst efficiency and facilitating catalyst recovery and reuse. Both pH and pH_{zcp} significantly influence the adsorption and photodegradation efficiency.

IM, an insecticide widely used in agricultural activities, is a neonicotinoid chemical. IM undergoes significant photolysis processes in water, and its hydrolysis half-life ranges from 33–44 days in a neutral solution at 25 °C. The IM is stable under acidic conditions.[16,48] The extensive use of IM poses hazards to aquatic ecosystems, necessitating the development of purification methods to mitigate these risks.[49–52]

Therefore, this work aimed to synthesize a ZnO@Ca-Alginate composite for use in the photodegradation of aqueous IM. The effects of pH and the effluent pHzcp on the equilibrium concentration of IM will be investigated, as well as the potential for complete mineralization. By elucidating these factors, we desire to develop viable and environmentally friendly methods for treating water contaminated with insecticides and other organic pollutants.

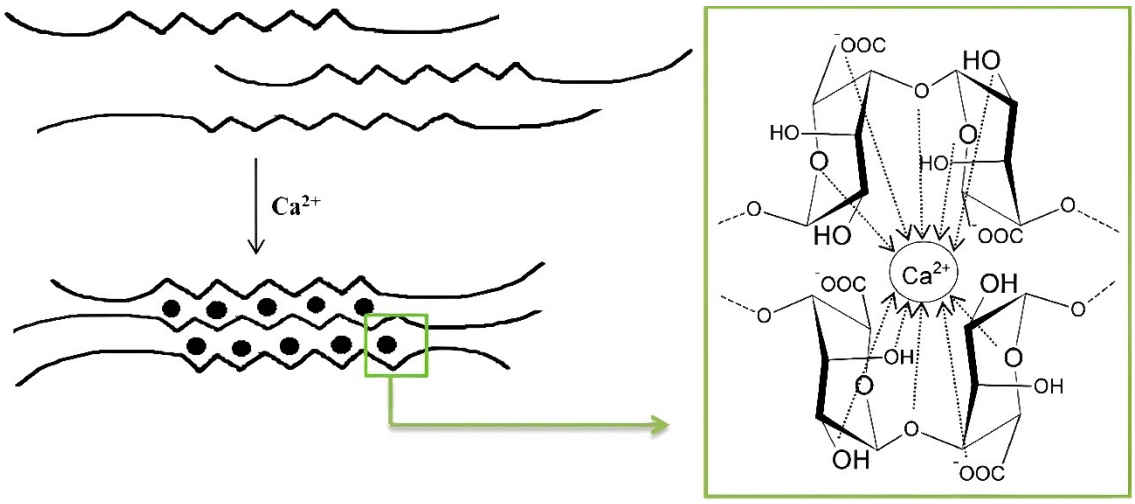

Figure 1. The repeating structure of Na-Alginate and the creation of an "egg-box" structure, which is formed by Ca^{2+} cations.[47]

Chemicals, Materials, and Methods

Chemicals

The chemicals used in this work were acquired from Sigma Aldrich (Darmstadt, Germany). These chemicals are sodium alginate (CAS No. 9005–38-3), Michigan, USA; methanol (CAS No. 67–56-1), Beijing, China; acetic acid (CAS No. 64–19-7), Ludwigshafen, Germany; $CaCl_2$ (CAS No. 10043–52-4), Texas, USA; acetonitrile (CAS No. 75–05-8), Missouri, USA; and zinc oxide (CAS No. 1314–13-2), Bremen, Germany. Acetic acid, methanol, and acetonitrile were used as HPLC solvents. IM was sourced from the local market for experimental use.

Composite Catalyst ZnO@Ca-Alginate Preparation

The following procedure was used to prepare the ZnO@Ca-Alginate composite, as described by Zyoud et al.[12] Initially, a 9.1% (w/w) ZnO suspension was prepared by stirring 20 g of ZnO nanopowder with 200 mL of distilled water. Two grams of Na-Alginate was dissolved in 100 mL of distilled water to prepare a 2% (w/w) solution of Na-Alginate. While vigorously stirring, the ZnO suspension was added to 100 mL of 2% (w/w) $CaCl_2$ solution. Simultaneously, Na-Alginate solution was added dropwise to the ZnO suspension with $CaCl_2$. Combining ZnO with the resulting insoluble Ca-Alginate formed a composite structure. The ZnO@Ca-Alginate composite was subsequently separated via suction filtration and dried in an oven at 100 °C for 3 hours, as shown in Scheme 1. The dried composite was maintained for further use. A photograph of the prepared ZnO@Ca-Alginate composite before and after drying is shown in Figure 2.

Catalyst Characterization

The X-ray diffraction (XRD) patterns of the composites were determined via a Philips XRD XPERT PRO diffractometer engineered by Philips (a renowned worldwide technology firm, Netherlands). The particle size within the developed composite was assessed via XRD patterns, and computations relied on the Scherer equation. ZnO@Ca-Alginate nanoparticle formation was confirmed through the observation of reflections in the XRD patterns. The composite morphology was examined by scanning electron microscopy (SEM) with a Jeol JSM-6700 F instrument manufactured by Jeol Ltd. (Japan). An FTIR spectrometer (Nicolet™ iS™ 5) from Thermo Scientific™, based in Massachusetts, USA, was used for further

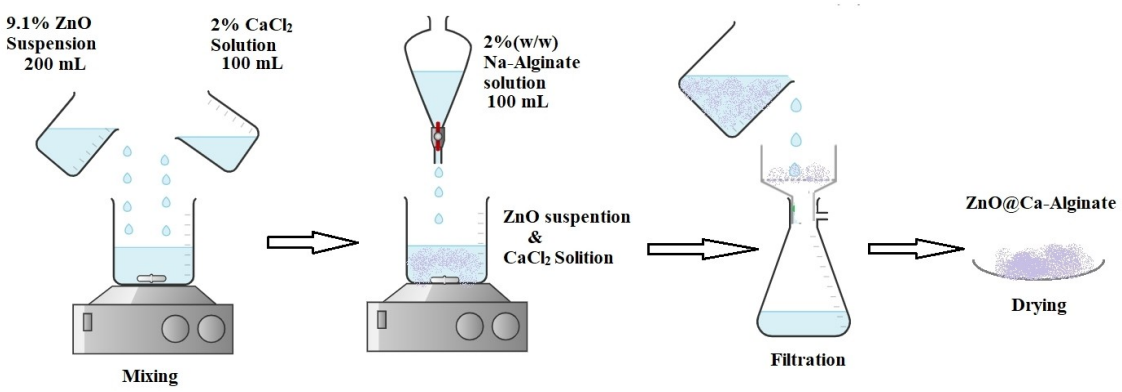

Scheme 1. Schematic diagram showing the preparation of ZnO@Ca-Alginate.

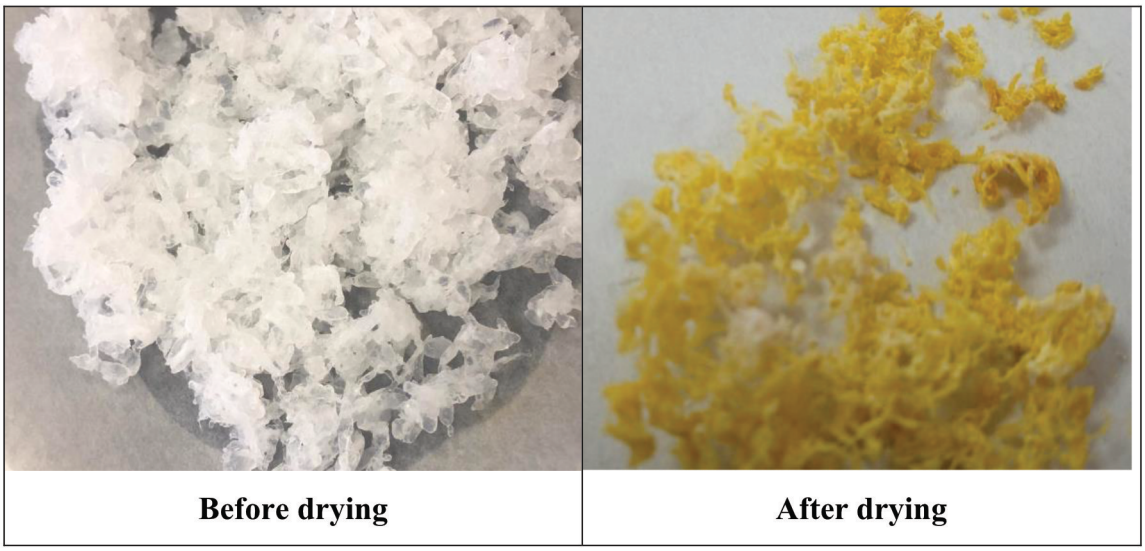

Figure 2. Pictorial photo of the prepared ZnO@Ca-Alginate photocatalyst before and after drying.

composite characterization and functional group identification. Additionally, an EDX complex composition analysis for determining each of the element proportions was performed with a Jeol JSM-6700 F scanning electron microscope. The transformation of the structure and stability of ZnO@Ca-Alginate were determined, and a TGA-1000 thermogravimetric analyzer produced by RT Instruments (California, USA) was utilized.

The pH at which the synthesized composite surface charge was zero (pHzcp) was determined via the pH drift method.[53] Initially, a 0.01 M NaCl solution was prepared, and the solution was then boiled to eliminate any dissolved gases, such as CO_2. A 50 mL aliquot of the NaCl solution was transferred to each of the six capped glass containers. The initial pH of the NaCl solution was modified by using drops of diluted solutions of HCl and/or NaOH in each container, and the containers were then purged with N_2 gas to eliminate any traces of dissolved CO_2. The solutions stored in these bottles were subsequently adjusted to initial pH values (pH_i) ranging from 2–12. Next, after 0.10 g of the catalyst was added to each bottle, the bottles were capped and shaken for 8 hours on a thermostatic shaker at 30 °C ±5. The final pH (pH_f) of the equilibrated solution was determined. The differences between pH_f and pH_i (ΔpH) were plotted against pH_i. The x-intercept indicates the pHzcp value of each catalyst.

Adsorption and Photocatalytic Experiments

The adsorption of IM onto ZnO@Ca-Alginate surfaces at various pH values was investigated. A series of batch studies were conducted, and each experiment involved four 200 mL beakers, each containing 0.10 g (containing 0.08 g of ZnO) of the prepared composite of ZnO@Ca-Alginate mixed with 50 mL of IM solution (40 ppm). The pH of the solutions in the beakers was adjusted to 4.5, 7, 9, or 12, and the temperature was maintained at 30 °C ± 5. After 30 minutes of continuous shaking, no significant loss of IM was observed at any adjusted pH. For further photodegradation experiments, a tungsten solar simulator lamp (0.015 w/cm^2) was subsequently positioned over the reaction beakers containing mixtures of different pH values postadsorption. Aliquots were extracted from the solution at specific time intervals and centrifuged at 6000 cycles/min for 5 min. An HPLC-DAD Water1525 chromatograph with a C18 column was used. The mobile phase was composed of acetonitrile and 0.01 % phosphoric acid at a ratio of 1 : 2, and the flow rate was 1 mL/min. The analysis was performed at a wavelength of 270 nm to determine the IM concentration, and the percentage of photodegraded IM was determined. The complete mineralization of IM as well as the determination of any intermediates during the photodegradation steps were verified via UV-visible spectrophotometric analysis and HPLC analysis for periodically aspirated samples at different photodegradation intervals. Additionally, the total organic carbon (TOC) in the aspirated samples was analyzed via a TOC-$L_{CSH/CPH}$ Shimadzu analyzer. The analysis was employed to prove the full mineralization of the IM. The composite catalyst efficiency after recovery and reuse was assessed by filtering, cleaning with distilled water, and drying to facilitate reuse following the photodegradation phase.

2. Results and Discussion

2.1. Characterization of the Composite Catalyst

Figure 3 displays the X-ray diffraction pattern of the ZnO nanopowder, revealing distinct peaks at 2θ angles of 31.87°, 34.52°, 36.35°, 47.52°, 56.57°, 62.93°, 66.44°, 68.03°, and 77.04° corresponding to the (100), (002), (101), (102), (110), (103), (200), (112), (201), and (202) Bragg planes, respectively.[54] Using the Scherrer equation, $D=K\lambda/\beta\cos\theta$, where K is the Scherrer constant, λ is the wavelength of the X-ray beam used (1.54,184 Å), β is the full width at half maximum (FWHM) of the peak, θ is the Bragg angle,[55] and the ZnO particle size was determined from 2θ values of 36.35°, 34.52°, and 31.87°, yielding an average particle size of 56 nm.

The X-ray diffraction pattern of Ca-Alginate in Figure 3 displays a broadened reflection ranging between 2θ angles of 10° and 20°. This broadening is an indication of a fine and small particle size. Reflections at 2θ angles of 15.63°, 14.16°, and 13.04° were used to estimate the particle size via the Scherrer equation, resulting in a calculated size of ~ 3 nm.

The primary peak reflections of ZnO (36.36°, 34.52°, and 31.87°) and Ca-Alginate (47.7° and 13.47°) remain unshifted in the spectrum, suggesting successful support of ZnO on the Ca-Alginate composite surface (Figure 3).

Figure 4 shows a scanning electron microscopy (SEM) image of ZnO@Ca-Alginate. This result confirmed the deposition of ZnO nanoparticles on the alginate surface, confirming the formation of the composite ZnO@Ca-Alginate system. The agglomerated bedded Ca-Alginate frameworks are comparable to those stated and reported in similar literature.[56,57]

The integration of Ca-Alginate into the composite was confirmed via EDX analysis. The elemental composition and percentage distribution of each element within the composites were analyzed. The EDX analysis results indicated the presence of Ca, C, Zn, and O in the prepared composite (Figure 5). The analysis revealed that the percentages of zinc and oxygen were greater than those of carbon and calcium. This finding aligns with the initial composition ratios employed during the preparation of the composite, which maintained a mass ratio of 1 : 4 for Ca-Alginate:ZnO. The percentage composition across the EDX analyses was determined to be 30.27 % for carbon, 43.56 % for oxygen, 0.39 % for calcium, and 25.78 % for zinc. These results for the Ca-Alginate composition are comparable with other reported results.[58]

2.1.1. FT-IR Spectroscopy Analysis of ZnO@Ca-Alginate

Figure 6 shows the FT-IR spectrum of pristine ZnO. The absorption band positioned at approximately 481 cm^{-1} corresponds to the Zn–O vibration mode.[59] Additional minor bands detected at 1162 cm^{-1} and 1301 cm^{-1} are attributed to atmospheric CO_2 absorption. Alginic acid, a copolymer created from a-L-guluronic acid (G) as well as 1,4-linked-b-D-mannuronic acid (M),[60] presents two separate absorption bands corresponding to each polymer.

The FT-IR spectra of sodium alginate and calcium alginate are presented in Figure 6. The absorption band at 823 cm^{-1} corresponds to the mannuronic acid vibration, whereas the absorption band at 1030 cm^{-1} corresponds to the guluronic acid C–O stretching vibration.[61,62]

The Ca-Alginate spectrum shows an absorption band that corresponds to the O–H vibration at approximately 3400 cm^{-1},

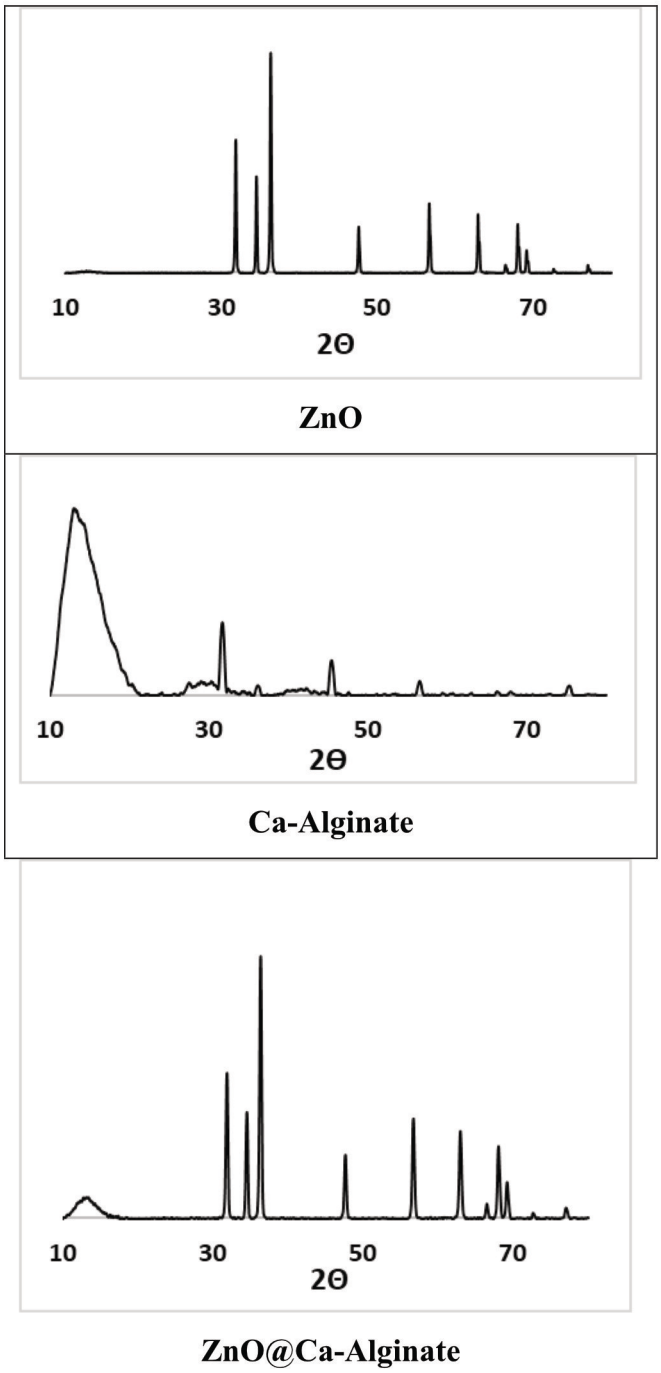

Figure 3. XRD patterns of ZnO, Ca-Alginate, and ZnO@Ca-Alginate.

which is wider than that of Na-Alginate. This widening is due to the decrease in the number of hydrogen bonds due to Ca^{2+} intercrosslinking. The involvement of Ca^{2+} in the coordination between the –COOH and –OH groups of alginates results in weakened vibration bands, as shown in Figure 6.

A comparison of the ZnO@Ca-Alginate nanocomposite spectrum with the spectra of Ca-Alginate and pristine ZnO is presented in Figure 6. Ca-Alginate contributes to bands at 973 cm^{-1}, 1432 cm^{-1}, and 1600 cm^{-1}, whereas the vibration band of Zn–O gives rise to 522 cm^{-1}.[63–65] The chemisorption process of ZnO onto the alginate layers produces a slight shift in the Zn–O absorption band toward a lower frequency.[66]

The TGA and DTG curves, which illustrate the thermal behavior of the ZnO@Ca-Alginate composite, are presented in Figure 7. Several distinct thermal events can be discerned from the DTG curve.

The initial loss, which was caused mainly by volatile substances such as water, occurred at 41–233 °C, resulting in a

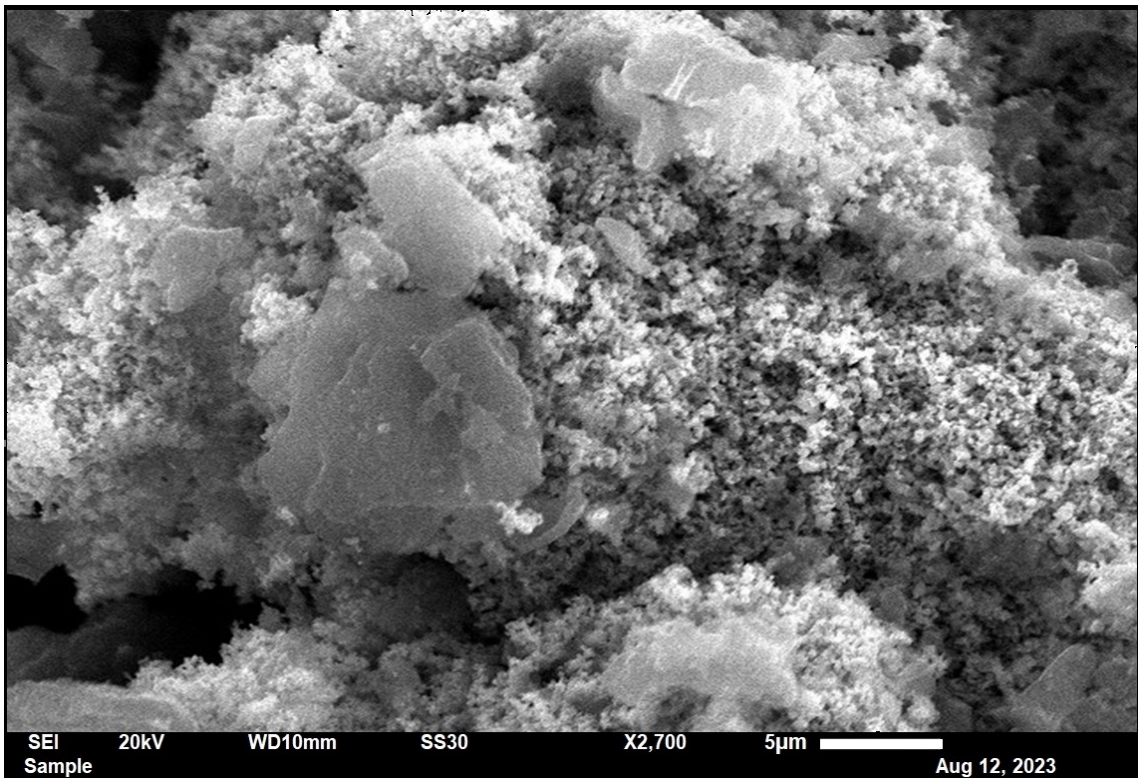

Figure 4. Scanning electron micrograph of ZnO@Ca-Alginate.

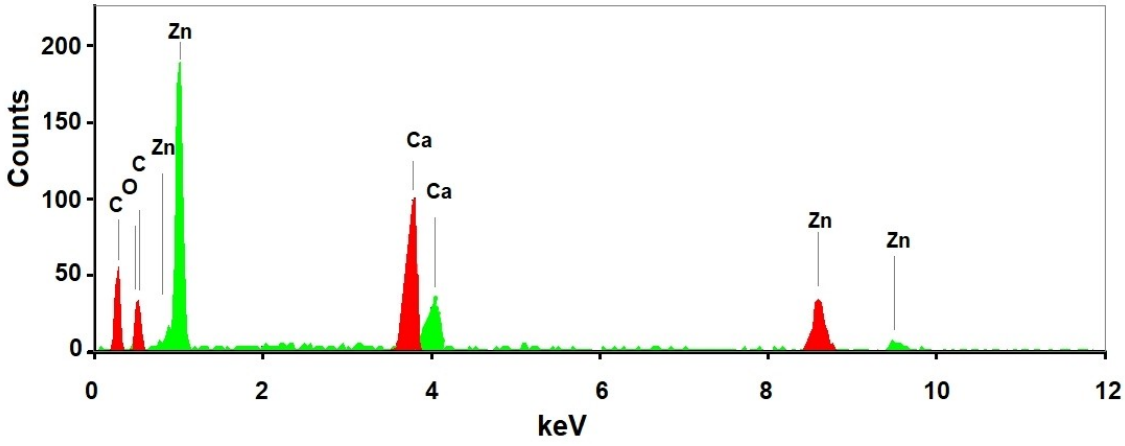

Figure 5. EDX spectra showing various elements in the prepared ZnO@Ca-Alginate composite.

6.2% loss. A 10.55% mass loss subsequently occurred through the next thermal degradation phase, which was observed at temperatures ranging between 150 and 350 °C.

The subsequent thermal degradation phase, occurring at temperatures ranging between 550 and 800 °C, led to a mass loss of approximately 13.2%. The remaining residue, which is mostly related to ZnO in addition to other formed oxides such as CaO, accounted for 70% of the prepared composite, and these results are comparable to those of other reported Ca-Alginate composites.[67,68]

2.2. Zero Charge Points (pH_{zcp}) of the Adsorbent

The surface charge of the adsorbent and the equilibrium structure of the contaminant molecules are pivotal factors influencing the adsorption process. Therefore, determining the point of zero charge (pHzcp) of the adsorbent is crucial. Figure 8a shows the pHzcp value, solid surface charge, and density of ZnO@Ca-Alginate with respect to pH. The determined pHzcp was found to be 6.8. This indicates that the solid surfaces have positive charges at pH values lower than 6.8, whereas they become negatively charged at pH values greater than 6.8. The reported pHzcp values are consistent with those

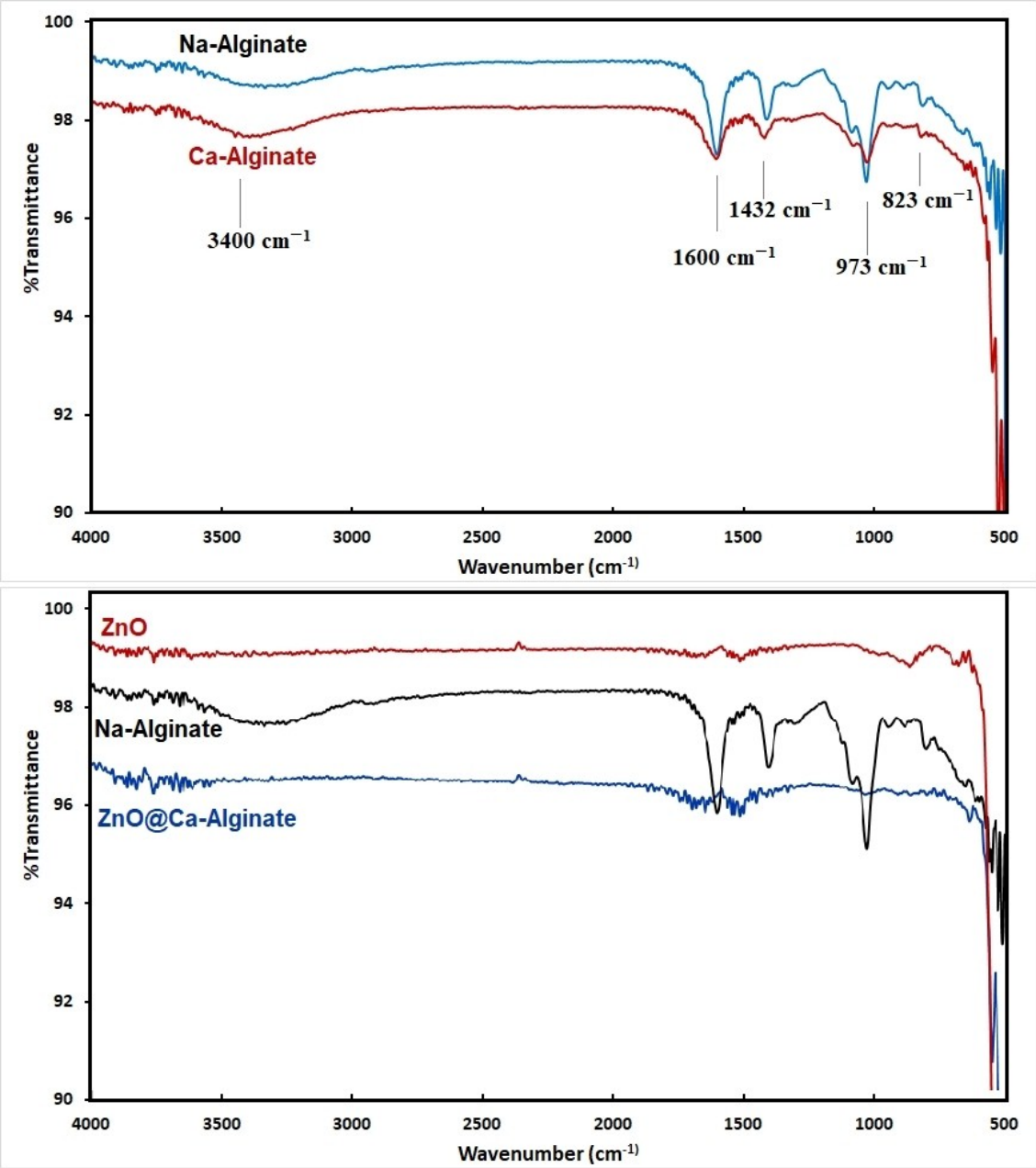

Figure 6. IR spectra of ZnO, Na-Alginate, Ca-Alginate, and ZnO@Ca-Alginate.

of other alginate composites.[69,70] The pHzcp of ZnO nanopowder is reported to be approximately 9.[12,71] Early studies have shown that the optimal pH for the degradation of most organic contaminants is within the basic range of approximately 9, which is significantly higher than the natural pH of water, which is approximately 7.[72–74] However, embedding ZnO nanoparticles within a Ca-Alginate composite shifted the pHzcp value to a lower value of 6.8. This shift enhances the photodegradation of IM under neutral pH conditions, which will be discussed in the following sections.

The IM (imidacloprid) has two predicted pKa values, which were calculated via Chemaxon software and were found to be 5.3 and 9.4. This suggests that the equilibrium structure of IM is predominantly positive when the pH is lower than 5.3, whereas it is predominantly negative when the pH is greater than 9.4. Within the pH range of 5.4–9.3, IM tends to maintain a mostly neutral charge.

In circumstances where the catalyst surface charge aligns or contrasts with the charge of IM molecules, electrostatic forces likely govern the process of adsorption or repulsion, subsequently influencing photodegradation. Conversely, in the scenario of a neutral equilibrium structure of IM, hydrogen bonding predominantly dictates the adsorption process, as depicted in Figure 8b.

The prepared ZnO@Ca-Alginate composite exhibited a specific surface area of 330 m^2/g, as determined by BET

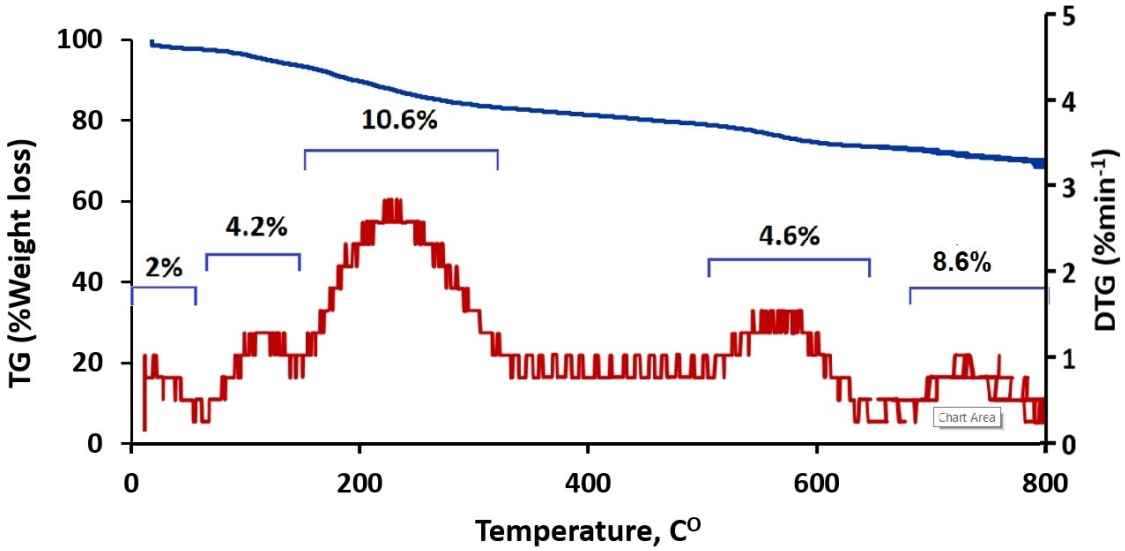

Figure 7. TGA and DTG plots of the ZnO@Ca-Alginate nanoparticles.[12]

(Brunauer-Emmett-Teller) analysis. This high surface area is indicative of the material's potential for efficient photocatalytic activity, as it provides more active sites for the degradation process, thereby enhancing the overall photocatalytic performance.

2.3. Adsorption and Photodegradation Findings

The chemical structure and functional groups of Ca-Alginate play crucial roles in influencing the adsorption process, as do the porosity and specific surface area. As depicted in Figure 9, the efficiency of IM photodegradation significantly increased at a pH of approximately 9 compared with that at pH 7, whereas the degradation rates notably decreased at pH 4.5 and pH 12.

IM primarily exists in a neutral form within the pH range of 5.5–9.5. Consequently, hydrogen bonding is anticipated to be the primary mechanism of adsorption within this pH range, as shown in Figure 9. At approximately pH 7, as depicted in region 2 (**R2**) of Figure 8, hydrogen bonding predominates between the neutral IM molecules (which are rich in N heteroatoms in the IM structure) and the –OH groups of the Ca-Alginate skeleton of the composite. This absence of repulsion between IM and the composite surface may result in a slightly decreased photodegradation efficiency compared with that at pH ~9, where the abundance of OH- ions in the solution serves as a source of hydroxyl radicals, thereby facilitating the photodegradation process, as depicted in region 3 (R3) of Figure 8.

At pH ~12, corresponding to region 4 (**R4**) in Figure 9, the IM molecules and the composite surfaces are negatively charged. This similarity in charge results in electrostatic repulsion, preventing IM molecules from approaching the catalyst surface, which is rich in hydroxyl radicals, thereby diminishing the photodegradation process.

At a low pH (~4.5), as depicted in region 1 (**R1**) of Figure 9, IM primarily exists as a positively charged species aligning with the positively charged surface of the composite catalyst. This similarity in charge induces repulsive forces that discourage IM molecules from reaching the catalyst surface, consequently reducing the photodegradation of IM.

The solution at pH 9 is noteworthy for its abundance of OH^- ions, which are essential for generating hydroxyl radicals ($^{\bullet}OH$), the most active species in the photodegradation process. This characteristic highlights the heightened efficiency of IM photodegradation at this pH, a trend that extends to the pH range associated with region 3 (**R3**) of neutral to slightly basic media, as shown in Figure 9. A neutral pH of 7 maintains effective photodegradation of IM, demonstrating comparable efficiency to the optimal pH value of 9. This finding highlights an advantageous feature of the prepared photocatalyst, as it performs well at neutral pH while maintaining efficacy comparable to the optimal pH. This property underscores the versatility and practical applicability of the photocatalyst under various environmental conditions.

2.4. Confirmation of Contaminant Mineralization

HPLC analysis was conducted at various irradiation intervals (0, 60, 120, and 180 min) to investigate the degradation and intermediates of IM (50 mL, 20 ppm). The reduction in the contaminant peak area along with the emergence of further peaks (intermediates) confirmed that contaminant degradation occurred.

In Figure 10, chromatogram (a) displays a prominent peak at $t_R = 2.4$ min, with a peak area of 2522966 μV.sec, representing 98% of the peak areas attributed to IM. After 60 min of irradiation, the chromatogram (b) reveals a peak at a t_R of 2.4 min with a peak area of 749336 μV.sec, whereas two new peaks emerge at a t_R of 2.1 min (peak area: 603304 μV.sec) and a t_R of 1.8 min (peak area: 404365 μV.sec), attributed to

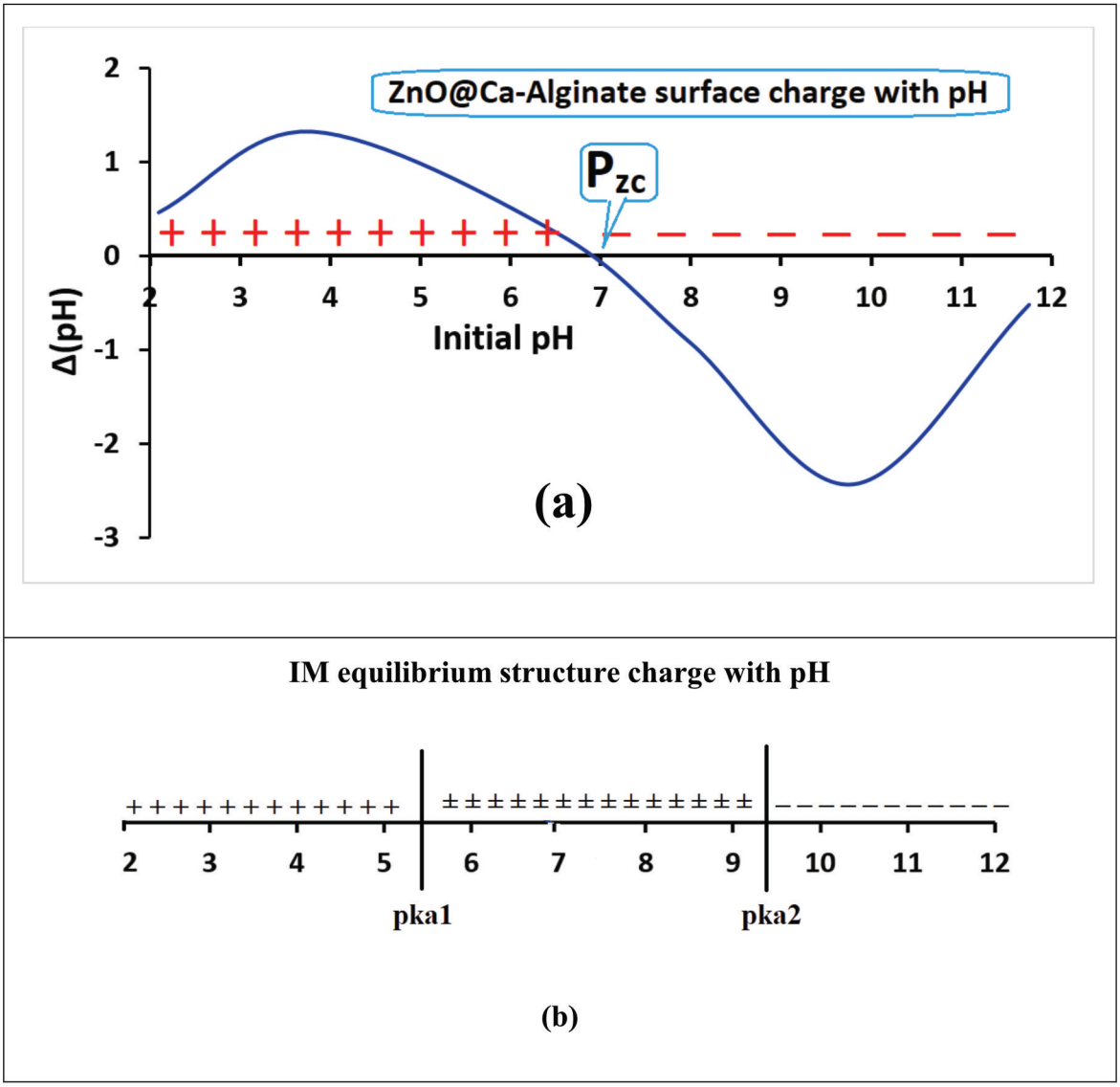

Figure 8. a) Plot of △(pH) vs. initial pH for ZnO@Ca-Alginate. The intercept shows the value of pHzcp for the solid. b) IM equilibrium structure charge with respect to pH.

intermediate product formation and chlorine ions, respectively.[70]

A chromatograph (c) following 120 min of irradiation revealed the disappearance of the peak at a t_R of 2.4 min, confirming complete IM degradation. Additionally, a decrease in the peak at a t_R of 2.1 min (peak area: 511883 μV.sec) is observed, as is an increase in the chlorine ion peak at a t_R of 1.8 min (peak area: 492853 μV.sec). After 180 min of irradiation, the chromatogram (d) exhibited an increase in the primary peak at a t_R of 1.8 min, attributed to chlorine ions.

TOC analysis confirmed the complete elimination of organic matter from the treated solution after 3 h of irradiation. The TOC values for samples taken at 0, 60, 120, and 180 minutes of irradiation were 8, 3.6, 1.5, and 0.5 ppm, respectively, indicating up to 94% mineralization of organic intermediates during the photodegradation process.

UV-visible spectroscopic measurements were performed on the aspirated samples at various intervals of degradation (0, 30, 60, 90, 120, 150, and 180 minutes). The resulting spectra are shown in Figure 11. The spectra reveal a gradual decrease in the IM absorption peak at 270 nm over time, with the peak almost disappearing after 180 minutes of irradiation, indicating complete degradation of the IM. Simultaneously, an absorption peak at approximately 300 nm begins to emerge and intensifies with increasing irradiation time. This peak is characteristic of nitrate ions (NO_3^-),[75] which are formed from the nitrogen atoms present in IM. Another absorption peak, observed at approximately 350 nm, also increased during the photodegra-

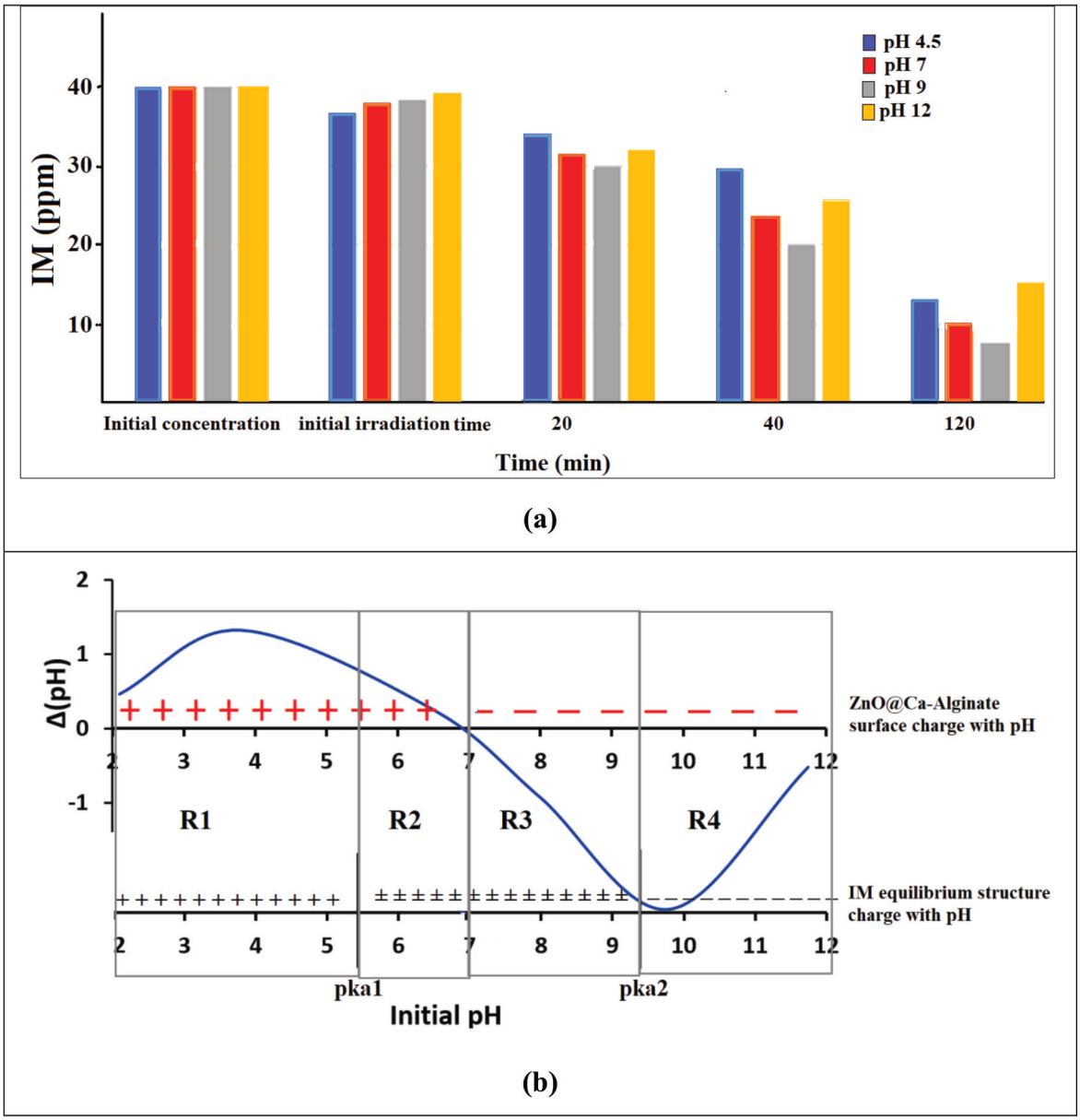

Figure 9. a) Effect of pH on the photodegradation of IM (50 mL, 20 ppm) using 0.10 g of ZnO@Ca-Alginate at different pH values (4.5, 7, 9, and 12). b) Regions in the pH range with a composite surface charge and IM equilibrium structure charge with respect to pH.

dation of IM. This peak corresponds to chloride ions (Cl_3^-)[76] generated from the chlorine atoms in IM.

In summary, a decrease in the IM concentration during photodegradation was indicated by the continued decrease in the peak retention time at 2.4 min. The peak at 2.1 min increased during photodegradation and then decreased, indicating complete degradation of the formed intermediates. The peak at ~1.8 min, which gradually increased during the photodegradation of IM, corresponded to the produced chloride ions.[77] The final products of IM photocatalytic degradation, including CO_2, Cl^-, N_2, and NO_3^-, were confirmed by HPLC, total organic carbon (TOC), and UV-Vis spectroscopic analyses. These final photodegradation products of IM are consistent with those reported in other studies.[70,78] Scheme 2 illustrates the suggested and proposed photodegradation pathway of IM to the final products CO_2, Cl^-, and NO_3^-.[48]

Recovery and reuse experiments were conducted to evaluate the efficiency of the ZnO@Ca-Alginate composite as a reusable photocatalyst. In these experiments, 0.1 g of the composite was mixed with 50 mL of a 40 ppm IM solution, which was adjusted to an optimal pH of 9. The solution was then exposed to direct irradiation for 120 minutes, followed by decanting the mixture. The extent of IM photodegradation was quantified via HPLC. This process was repeated four times, with fresh IM solutions each time, maintaining the pH at 9 and subjecting the mixture to the same irradiation conditions.

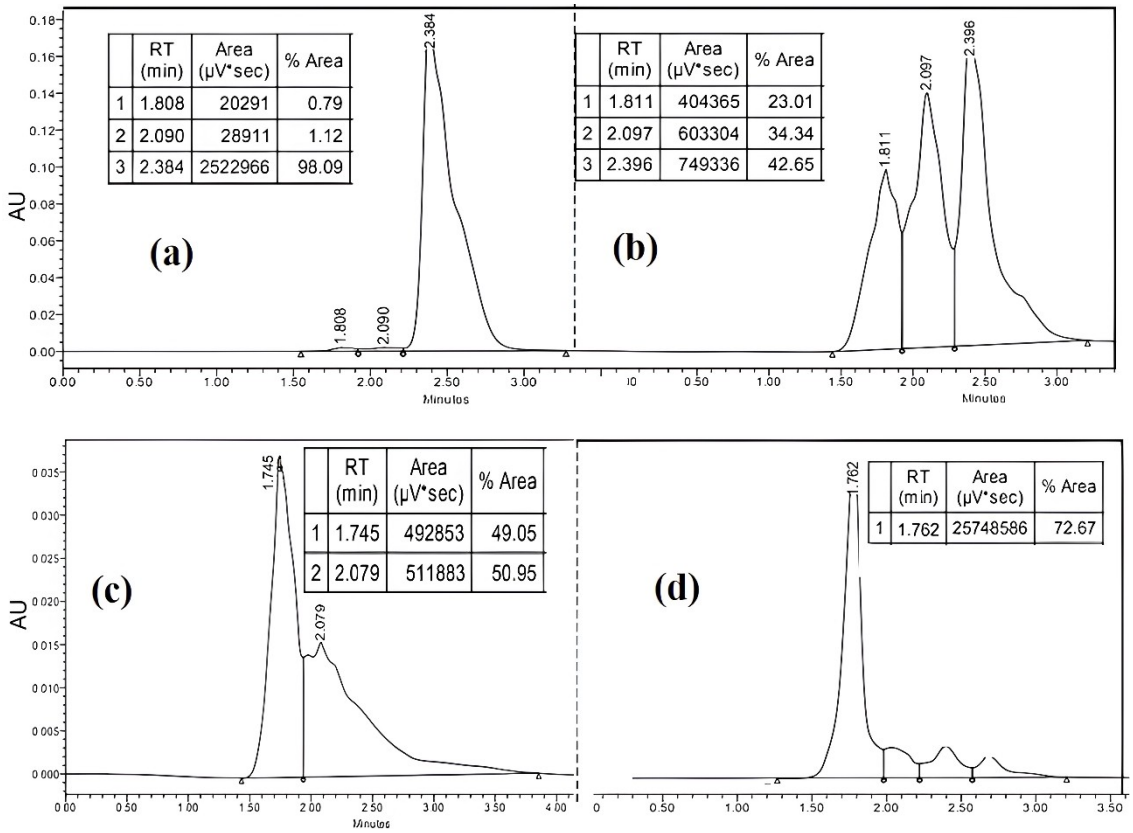

Figure 10. HPLC chromatogram analysis of IM (50 mL, 20 ppm) with 0.10 g of catalyst at various irradiation times: a) 0, b) 60 min, c) 120 min, and d) 180 min, pH 9, 30 °C ± 5.

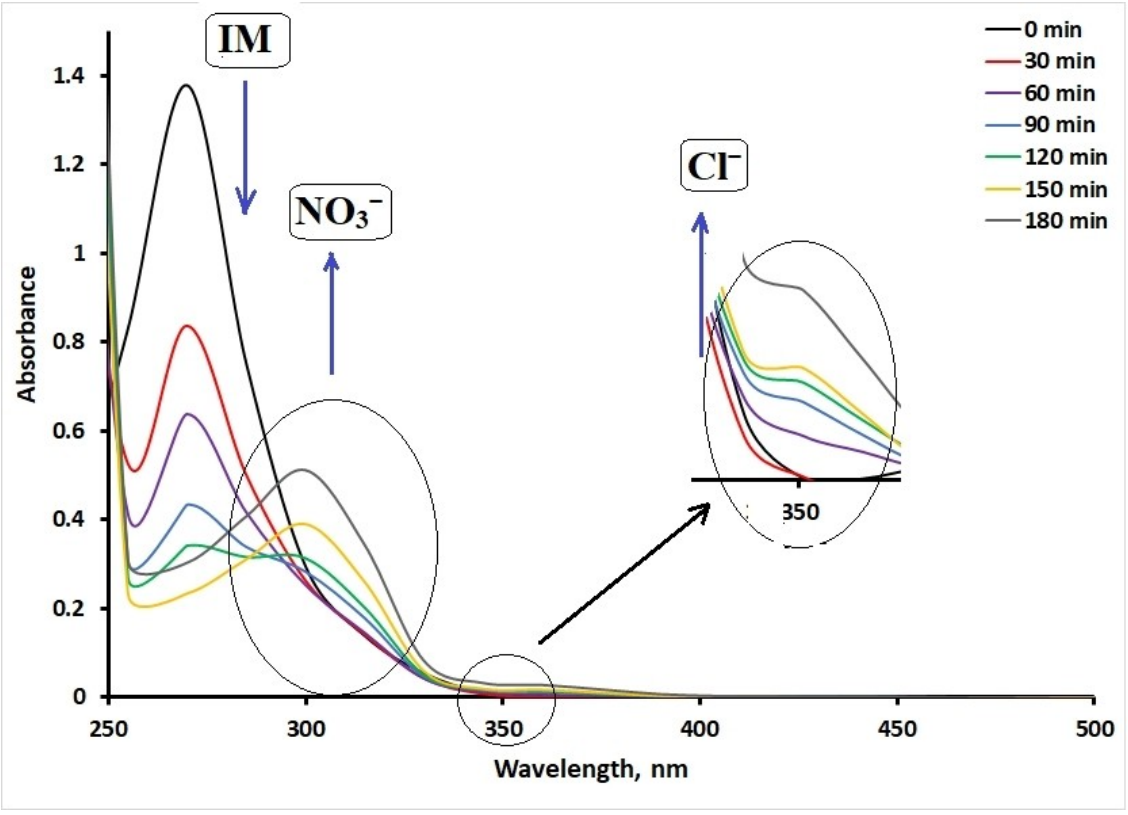

Figure 11. UV-visible spectroscopic profiles of the IM solution were analyzed after various photodegradation time intervals.

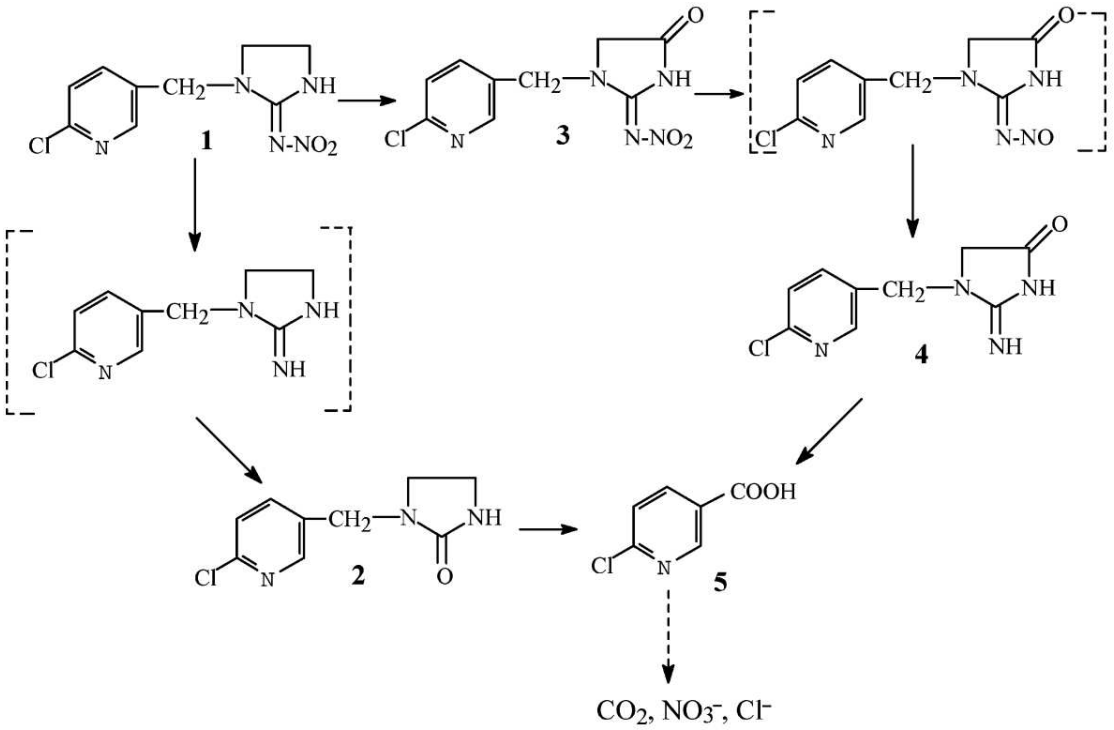

Scheme 2. Major photolysis processes of IM in water.[48]

The photodegradation efficiency during each irradiation cycle was 82%, 79%, 80%, and 77%, respectively. These results indicate that the photocatalyst retained a high level of efficiency across multiple cycles, with only a minor decrease in performance. The consistent degradation rates suggest that the ZnO@Ca-Alginate composite is highly effective in the photodegradation process and has excellent reusability.

The slight variation in efficiency across cycles can be attributed to minor losses in active sites or possible adsorption of byproducts on the catalyst surface, but overall, the performance remains robust. The ease of catalyst recovery after each cycle, combined with its sustained efficiency, highlights the practical advantages of using this composite in sustainable photocatalysis processes. This makes the ZnO@Ca-Alginate composite a cost-effective and environmentally friendly option for repeated use, offering significant potential for practical applications in environmental remediation.

In this study, the ZnO@Ca-Alginate composite catalyst demonstrated a 94% photodegradation efficiency of imidacloprid (IM) under solar-simulated light after 180 minutes. This performance is notably higher than that of many reported studies under varying conditions. For example, TiO_2 and ZnO catalysts under UV irradiation achieved 88% and 82% efficiency in 20 minutes for 100 ppm IM solutions, respectively. However, these results were obtained under UV light, which is less environmentally friendly than solar-simulated light is. Similarly, CdS under solar-simulated light achieved only 70% degradation in 90 minutes for a 10 ppm IM solution, indicating that ZnO@Ca-Alginate is more efficient. Although graphene-C_3N_4 and g-C_3N_4/TiO_2 achieved high efficiencies (90%) under visible light, they required longer irradiation times (150–300 minutes). Therefore, the high efficiency of ZnO@Ca-Alginate under more sustainable solar-simulated light, coupled with its competitive degradation time, makes it a superior photocatalyst for IM degradation (Table 1).

3. Conclusions

This study demonstrated the successful application of ZnO@Ca-Alginate composites for the photocatalytic degradation of imidacloprid (IM). The synthesis of the composite, which integrates ZnO nanoparticles into a Ca-Alginate matrix, resulted in a highly effective photocatalyst for breaking down the IM. The ZnO@Ca-Alginate composite achieved complete mineralization of IM into CO_2, Cl^-, N_2, and NO_3^- within 3 hours of irradiation. The optimal degradation efficiency was observed at a pH of 9, where a high concentration of hydroxyl radicals facilitated the breakdown of IM. The study identified a point of zero charge (pHzcp) for the composite at 6.8, which shifted the optimal pH for degradation to a more neutral range than that of pure ZnO. This shift enhances the photocatalytic performance under typical environmental conditions. Additionally, the composite demonstrated robust stability, with high photocatalytic efficiency maintained over four reuse cycles. These findings underscore the practical advantages of using ZnO@Ca-Alginate in sustainable water treatment applications, offering a cost-effective and environmentally friendly solution for repeated use in the remediation of contaminated water.

Table 1. Comparison of the photodegradation efficiency of IM with other reported studies under different catalysts and conditions.

IM, V, Con. (ppm)	Catalyst dose (g)	Irradiation Type	Time of irradiation (min)	Efficiency %	Ref
100 mL, 100 ppm	TiO_2 (0.1 g)	UV lamp	20	88%	[79]
100 mL, 100 ppm	ZnO (0.1 g)	UV lamp	20	82%	[79]
100 mL, 20 ppm	TiO_2, Fe^{3+}, H_2O_2 (0.5 g)	UV lamp	60	64%	[80]
100 mL, 20 ppm	ZnO (0.5 g)	UV lamp	60	80%	[80]
500 mL, 10 ppm	TiO_2 (1 g)	UV lamp	40	94%	[81]
50 mL, 10 ppm	CdS (0.05 g)	Solar simulated light	90	70%	[82]
100 mL, 20 ppm	graphene-C_3N_4 (0.05 g)	Visible	300	90%	[83]
450 mL, 10 ppm	TiO_2 (10 g), Thin film	UVA	240	83%	[84]
10 mL, 10 ppm	g-C_3N_4/TiO_2 (0.01 g)	Tungsten lamp	150	90%	[85]
1 L, 100 ppm	ZnO (1 g)	Sun light	42	50%	[86]
1 L, 100 ppm	ZnO/H_2O_2 (1 g)	Sun light	149	50%	[86]
5 mL, 10 ppm	ZnO (0.05 g)	Visible	60	56%	[87]
5 mL, 10 ppm	$CoFe_2O_4$ (0.05 g)	Visible	60	58%	[87]
5 mL, 10 ppm	ZnO/$CoFe_2O_4$ (0.05 g)	Visible	60	75%	[87]
50 mL, 20 ppm	ZnO@Ca-Alginate (0.1 g)	Solar simulated light	180	94%	This work

Author Contributions

The findings presented in this study were drawn partly from A. Z.'s thesis,[88] which was supervised by H. S. H. and A. H. Z. Additional results were obtained via A.H. Z. SEM and EDS, and additional XRD measurements were conducted by S. Z. and N. Q. at the laboratories of UAE University. Sh. H. Z. contributed to the TOC analysis. A. H. Z. and Sh. H.Z. collaborated on the drafting of the manuscript. All the authors reviewed and approved the final version of the manuscript. The Middle East Desalination Research Center (MEDRC) and > Palestinian Water Authority funded the master's student Ahlam Zyoud during her master's study.

Conflict of Interests

The authors declare no conflict of interest.

Data Availability Statement

This study does not involve applicable data sharing.

Keywords: Photocatalysis · Na-Algenite · Point of zero charge · Imidacloprid degradation · Sustainable water treatment

[1] A. Mukhopadhyay, S. Duttagupta, A. Mukherjee, *J. Environ. Chem. Eng.* **2022**, *10*(3), 107560.
[2] D. M. Mackay, P. V. Roberts, J. A. Cherry, *Environ. Sci. Technol.* **1985**, *19*(5), 384–392.
[3] P. H. Gleick, *Dirty-water: estimated deaths from water-related diseases 2000–2020*, Citeseer, **2002**.
[4] M. Pal, et al., *Air Water Borne Dis.* **2018**, *7*(1000138), 2.
[5] T. Benhalima, W. Chicha, H. Ferfera-Harrar, *Int. J. Biol. Macromol.* **2023**, *253*, 127532.
[6] H. Ferfera-Harrar, T. Benhalima, D. Lerari, *Int. J. Mater. Metall. Eng.* **2020**, *14*(1), 5–15.
[7] T. Benhalima, A. Sadi, N. Dairi, H. Ferfera-Harrar, *Sep. Purif. Technol.* **2024**, *342*, 127001.
[8] A. H. Zyoud, S. H. Zyoud, A. Amireh, *Case Studies in Chem. Environ. Eng.* **2024**, *9*, 100631.
[9] R. Rashid, et al., *Environ. Sci. Pollut. Res.* **2021**, *28*, 9050–9066.
[10] M. C. van Loosdrecht, P. H. Nielsen, C. M. Lopez-Vazquez, D. Brdjanovic, *Experimental methods in wastewater treatment*, IWA publishing, **2016**.
[11] H. S. Hilal, et al., *Solid State Sci.* **2010**, *12*(4), 578–586.
[12] A. Zyoud, et al., *Environ. Sci. Pollut. Res.* **2023**, *30*(26), 68435–68449.
[13] I. Badran, R. Khalaf, *Sep. Sci. Technol.* **2020**, *55*(14), 2433–2448.
[14] Y. M. Hunge, et al., *J. Photochem. Photobiol. A Chem.* **2023**, *434*, 114250.
[15] N. A. Oladoja, et al., *Environ. Sci. Pollut. Res.* **2023**, *30*(33), 80545–80558.
[16] T. Tišler, A. Jemec, B. Mozetič, P. Trebše, *Chemosphere.* **2009**, *76*(7), 907–914.
[17] S. Kagabu, S. Medej, *Biosci. Biotechnol. Biochem.* **1995**, *59*(6), 980–985.
[18] H. Wamhoff, V. Schneider, *J. Agric. Food. Chem.* **1999**, *47*(4), 1730–1734.
[19] T. H. Pham, et al., *Environ. Res.* **2023**, *217*, 114825.
[20] F. Z. Janani, et al., *Environ. Sci. Pollut. Res.* **2023**, *30*(34), 81403–81416.
[21] T. Benhalima, F. Z. Allali, N. Roumane, H. Ferfera-Harrar, *J. Mol. Liq.* **2023**, *383*, 122150.
[22] T. Benhalima, H. Ferfera-Harrar, N. Saha, P. Saha, *J. Macromol. Sci., Part A.* **2023**, *60*(6), 442–461.
[23] A. H. Zyoud, et al., *J. Environ. Chem. Eng.* **2020**, *8*(5), 104227.
[24] J. Liu, et al., *Environ. Sci. Pollut. Res.* **2023**, *30*(4), 9738–9748.
[25] A. Kumar, et al., *Environ. Res.* **2023**, *216*, 114741.
[26] M. Priyadarshini, I. Das, M. M. Ghangrekar, L. Blaney, *J. Environ. Manage.* **2022**, *316*, 115295.
[27] C. Zou, et al., *Environ. Sci. Pollut. Res.* **2019**, *26*, 1315–1322.
[28] A. Mittal, V. Thakur, V. Gajbe, *Environ. Sci. Pollut. Res.* **2013**, *20*, 260–269.
[29] I. Badran, M. O. Al-Ejli, *ChemistrySelect.* **2022**, *7*(38), e202202976.
[30] T. Benhalima, M. Mokhtari, H. Ferfera-Harrar, *J. Water Process Eng.* **2024**, *57*, 104670.
[31] A. Zyoud, et al., *Solid State Sci.* **2011**, *13*(6), 1268–1275.
[32] M. M. Halmann, *Photodegradation of water pollutants*, CRC press, **1995**.
[33] A. H. Zyoud, et al., *JOM.* **2021**, *73*, 404–410.
[34] A. Zyoud, et al., *Solid State Sci.* **2017**, *74*, 131–143.
[35] A. K. Dey, S. R. Mishra, M. Ahmaruzzaman, *Environ. Sci. Pollut. Res.* **2023**, *30*(18), 53887–53903.
[36] T. Saad Algarni, N. A. Abduh, A. Al Kahtani, *A. Aouissi, Green Chem. Lett. Rev.* **2022**, *15*(2), 460–473.
[37] F. G. Nunes Filho, et al., *Appl. Clay Sci.* **2023**, *239*, 106952.
[38] J. Tang, et al., *Chemosphere* **2023**, *335*, 139048.
[39] S. Mallakpour, E. Azadi, M. Dinari, *Carbohydr. Polym.* **2023**, *301*, 120362.
[40] H. Hecht, S. Srebnik, *Biomacromolecules* **2016**, *17*(6), 2160–2167.

[41] K. I. Draget, G. Skjåk-Bræk, O. Smidsrød, *Int. J. Biol. Macromol.* **1997**, *21(1-2)*, 47–55.
[42] P. A. Fufa, et al., *Nanotechnology* **2022**, *33*(31), 315601.
[43] M. Nawaz, et al., *Carbohydr. Polym.* **2018**, *199*, 109–118.
[44] B. Taghiloo, A. Shahnazi, M. R. Nabid, *J. Alloys Compd.* **2024**, 175859.
[45] M. F. Valiyathur, A. A. Raza, A. B. Kottur, M. S. Sakvai, *Carbohydr. Polym.* **2024**, *343*, 122431.
[46] M. Zendehzaban, M. Ashjari, S. Sharifnia, *Int. J. Energy Res.* **2020**, *44*(3), 2150–2163.
[47] A. Łętocha, M. Miastkowska, E. Sikora, *Polymers (Basel).* **2022**, *14*(18), 3834.
[48] W. Liu, W. Zheng, Y. Ma, K. K. Liu, *J. Environ. Sci. Health, Part B.* **2006**, *41*(5), 623–634.
[49] R. Nugnes, et al., *Environ. Pollut.* **2023**, *316*, 120682.
[50] D. Kathuria, M. Bhattu, A. Bankar, P. Puri, *ChemistrySelect* **2023**, *8*(34), e202302293.
[51] S. Stehle, et al., *Sci. Total Environ.* **2023**, *867*, 161383.
[52] J. Hou, C. Hu, L. Yang, X. Wang, *Mar. Pollut. Bull.* **2024**, *199*, 116013.
[53] D. W. Bahnemann, C. Kormann, M. R. Hoffmann, *J. Phys. Chem.* **1987**, *91*(14), 3789–3798.
[54] M. R. Arefi, S. Rezaei-Zarchi, *Int J Mol Sci.* **2012**, *13*(4), 4340–4350.
[55] I. Fatimah, S. Wang, D. Wulandari, *Appl. Clay Sci.* **2011**, *53*(4), 553–560.
[56] N. Yang, et al., *Crystals.* **2019**, *9*(5), 255.
[57] A. Borgiallo, R. Rojas, *ChemEngineering.* **2019**, *3*(1), 22.
[58] J. Liao, et al., *ACS Omega.* **2017**, *2*(2), 443–454.
[59] Z. Yang, Z. Ye, Z. Xu, *Physica E.* **2009**, *42*(2), 116–119.
[60] N. Chandıa, B. Matsuhiro, A. Vásquez, *Carbohydr. Polym.* **2001**, *46*(1), 81–87.
[61] H. Daemi, M. Barikani, *Scientia Iranica.* **2012**, *19*(6), 2023–2028.
[62] K. Essifi, et al., *Polym. Bull.* **2021**, *78*, 5789–5814.
[63] Z. N. Kayani, et al., *Materials Science-Poland.* **2015**, *33*(3), 515–520.
[64] M. H. Habibi, M. Mardani, *Spectrochim. Acta, Part A.* **2015**, *137*, 267–270.
[65] S. Ullah, et al., *Am. J. Phys. Sci.* **2024**, *2*(1), 1–25.
[66] C. D. Ene, et al., *Appl. Surf. Sci.* **2022**, *580*, 152231.
[67] S. Lin, et al., *Environ. Sci. Pollut. Res.* **2023**, *30*(29), 73534–73547.
[68] M. A. Rahman, et al., *Materialia.* **2020**, *13*, 100839.
[69] T. U. Rehman, et al., *RSC Adv.* **2019**, *9*(68), 40051–40061.
[70] N. Yasir, et al., *Polymers (Basel).* **2022**, *14*(5), 984.
[71] G. Yashni, A. Al-Gheethi, R. Mohamed, M. Al-Sahari, *Water Pract Technol.* **2020**, *16*, 364–376.
[72] A. H. Zyoud, et al., *Appl. Clay Sci.* **2019**, *182*, 105294.
[73] A. Zyoud, et al., *Int. J. Environ. Sci. Technol.* **2019**, *16*, 6267–6276.
[74] A. H. Zyoud, et al., *J. Environ. Chem. Eng.* **2020**, *8*(4), 104038.
[75] N. L. Aluker, M. Herrmann, Y. M. Suzdaltseva, *Opt. Spectrosc.* **2019**, *127*, 991–996.
[76] R. T. Sant'Anna, et al., J. Braz, *Chem. Soc.* **2012**, *23*, 1543–1550.
[77] S. R. R. Asaad, Clay-supported sensitized nano-ZnO in photocatalytic degradation of aqueous halophenols using direct solar light, An-Najah National University, **2018**.
[78] M. Kanwal, S. R. Tariq, G. A. Chotana, *Environ. Sci. Pollut. Res.* **2018**, *25*, 27307–27320.
[79] K. Yari, et al., *J. Environ. Health Sci. Eng.* **2019**, *17*, 337–351.
[80] V. Kitsiou, N. Filippidis, D. Mantzavinos, I. Poulios, *Appl. Catal., B* **2009**, *86(1-2)*, 27–35.
[81] J. Tang, et al., *Environ. Earth Sci.* **2012**, *66*, 441–445.
[82] H. Targhan, et al., *Sci Rep.* **2024**, *14*(1), 530.
[83] X. Liu, et al., J. Agric, *Food. Chem.* **2015**, *63*(19), 4754–4760.
[84] K. Babić, et al., *J. Environ. Chem. Eng.* **2021**, *9*(4), 105611.
[85] T. Kobkeatthawin, et al., *Catalysts.* **2022**, *12*(2), 120.
[86] A. Derbalah, et al., *J. Water Health.* **2019**, *17*(2), 254–265.
[87] M. Naghizadeh, M. A. Taher, A.-M. Tamaddon, *Heliyon.* **2019**, *5*(11).
[88] A. Zyoud, *Photocatalytic Degradation of Aqueous Methylene Blue and Imidacloprid by Ca Alginate-Supported ZnO Nanoparticles*, in *Chemistry M.Sc. Thesis*, An-Najah National University, Nablus, Palestine, **2021**.

Manuscript received: July 13, 2024